

On second-order combinatorial algebraic time-delay interferometry

Wei-Liang Qian^{2,1,3,*}, Pan-Pan Wang^{4,†}, Zhang-Qi Wu⁴, Cheng-Gang Shao⁴, Bin Wang^{1,5}, and Rui-Hong Yue¹

¹ Center for Gravitation and Cosmology, College of Physical Science and Technology, Yangzhou University, Yangzhou 225009, China

² Escola de Engenharia de Lorena, Universidade de São Paulo, 12602-810, Lorena, SP, Brazil

³ Faculdade de Engenharia de Guaratinguetá, Universidade Estadual Paulista, 12516-410, Guaratinguetá, SP, Brazil

⁴ MOE Key Laboratory of Fundamental Physical Quantities Measurement,

Hubei Key Laboratory of Gravitation and Quantum Physics, PGMF, and School of Physics,

Huazhong University of Science and Technology, Wuhan 430074, China and

⁵ School of Aeronautics and Astronautics, Shanghai Jiao Tong University, Shanghai 200240, China

(Dated: Oct. 1st, 2022)

Inspired by the combinatorial algebraic approach proposed by Dhurandhar *et al.*, we propose two novel classes of second-generation time-delay interferometry (TDI) solution as well as their further generalization. The primary strategy of the algorithm is to enumerate specific types of residual laser frequency noise associated with second-order commutators in products of time-displacement operators. The derivations are based on analyzing the delay time residual when expanded in time derivatives of the armlengths order by order. It is observed that the solutions obtained by such a scheme are primarily captured by the geometric TDI approach and therefore possess an intuitive interpretation. Nonetheless, the fully-symmetric Sagnac and Sagnac-inspired combinations inherit the properties from the original algebraic approach, and subsequently lie outside of the scope of geometric TDI. Moreover, at its lowest order, the solution is furnished by commutator of rather compact form. Besides the original Michelson-type solution, we elaborate on other types of solutions such as the Monitor, Beacon, Relay, Sagnac, fully-symmetric Sagnac, and Sagnac-inspired ones. The average response functions, residual noise power spectral density, and sensitivity curves are evaluated for the obtained solutions. Also, the relations between the present scheme and other existing algorithms are discussed.

I. INTRODUCTION

The TDI algorithm was first introduced by Tinto *et al.* [1] to suppress laser frequency noise in space-borne gravitational wave detectors [2–4]. The solution is formulated using a proper combination of the delayed science data stream, effectively constructing a virtual equal-arm interferometer [5]. Analogic to the original Michelson interferometer, most TDI solution possesses an intuitive geometric interpretation, which gives rise to the so-called geometric TDI approach [6]. From the algebraic perspective, the first-generation TDI [7, 8], associated with rigid armlengths, the solution space is a polynomial ring \mathcal{R} in three [9] and six [10] variables over the rational numbers. In particular, the problem can be reformulated to solve for the first *module of syzygies* of a left ideal of the ring [9, 10] using the notion of Groebner basis [11] in computational algebra.

On the other hand, the second-generation TDI takes into account the nonrigid rotation of the three-spacecraft constellation [12]. While expressing the residual noise as an expansion in terms of time derivatives of the armlengths, the cancelation scheme is effectively truncated at the second order. As a result, it provides a higher precision when compared to its first-generation counterpart. From the algebraic perspective, the time-delay operators, which constitute the variables of the polynomial, can no longer be considered commutative. The derivations of the second-generation TDI solutions are not straightforward. In practice, the geometric TDI, a method of exhaustion, is employed chiefly to seek feasible TDI combinations by enumerating all possible close trajectories in the space-time diagram [6, 13, 14]. Nonetheless, the solution space of the geometric TDI rapidly grows by 3^n , where n is the number of links, and therefore, the approach is computationally expensive at higher orders. Also, its relevant solution space is somewhat restrictive since a feasible solution demands that successive transmissions of laser signals must be physically associated with neighboring links. For instance, it is well-known that the fully symmetric Sagnac TDI solutions lie beyond such a solution space.

In the framework of the second-generation TDI, the use of the algebraic approach is somewhat restrictive, owing to its non-commutative nature. A notable exception is the combinatorial algebraic algorithm proposed by Dhurandhar *et al.* [15]. The original scheme mainly aimed for the Michelson-type scenario where one arm of the detector becomes

* E-mail: wlqian@usp.br

† E-mail: ppwang@hust.edu.cn

temporarily dysfunctional. Recently, the scheme has been extended to deal with a broadened selection of second-generation TDI combinations [16]. Mathematically, the TDI solution is furnished by the kernel of the following homomorphism associated with a polynomial ring \mathcal{R} in four variables

$$\varphi : \mathcal{R}^2 \rightarrow \mathcal{R}. \quad (1)$$

The proposed algorithm is based on the properties of a specific commutator between two monomials defined by the products of particular time-displacement operators. The algorithm essentially resides in the following three propositions. First, there is a specific class of commutators that vanishes when one only considers the first-order contributions regarding the time derivatives of the armlengths. Second, these commutators belong to the solution space of the second-generation TDI combinations. Last but not least, they are identical to the residual laser frequency noise of the corresponding TDI solution. In other words, by adequately enumerating (e.g., in the lexicographic order) such commutators, one manages to construct specific classes of TDI solutions systematically. The crucial feature of the extended algorithm proposed by some of us [16] is to include time-advance operators into the existing propositions. Subsequently, the approach can be applied to seek TDI solutions of the Monitor, Beacon, Relay, Sagnac, and fully symmetric Sagnac types. Moreover, a novel set of Sagnac-inspired solutions was derived, which cannot be straightforwardly obtained using the geometric TDI.

Compared to the method of exhaustion, an algebraic approach is beneficial because of its computational efficiency. Moreover, it scrutinizes the solution space and potentially furnishes us with a better understanding of the relevant module of the non-commutative ring. Therefore, further exploration regarding the relationship between the commutators of the time-displacement operators and second-generation TDI solutions is a worthy topic. The present study is motivated by the above considerations. It further generalizes the combinatorial algebraic approach to include two novel classes of second-generation TDI solutions. This is achieved by elaborating on two forms of residual laser noise associated with second-order commutators between polynomials in time-translation operators. As elaborated below, the associated residual laser noise manifestly vanishes regarding the contributions of first-order in the time derivatives of the armlengths. The first class of TDI solutions involves the commutator between a polynomial and an arbitrary commutator. In particular, the vanishing condition for the commutator imposed for the original algorithm is lifted: two monomials of equal length are replaced by two arbitrary polynomials. The second class is featured by the products of two polynomials in time-translation operators as its variables. We show that the derived second-generation TDI solutions are not included in the original algebraic approach or its recent generalization. While compared with those obtained before, the lowest-order solutions are furnished by commutators of a relatively compact form. Also, some of the solutions do not possess a straightforward geometric TDI interpretation.

The remainder of this letter is organized as follows. In Sec. II, we briefly review the TDI algorithm and present the utilized notations and conventions. The combinatorial approach proposed by Dhurandhar *et al.* and its recent generalization are also revisited. In Sec. III, we present the two novel classes of second-order TDI solutions. We elaborate on the forms of the residual laser noise and the procedure to derive the corresponding TDI coefficients. Subsequently, in Sec. IV, we explore various classes of solutions, namely, the Michelson, Monitor, Beacon, Relay, Sagnac, fully-symmetric Sagnac, and Sagnac-inspired ones. The average response functions, residual noise power spectral density, and the sensitivity curves of the obtained novel solutions are evaluated. The concluding remarks are given in the last section. The complementary mathematical derivations will be relegated to the Appendices A, B, and C.

II. TDI ALGORITHM AND THE FIRST-ORDER COMBINATORIAL ALGEBRAIC APPROACH

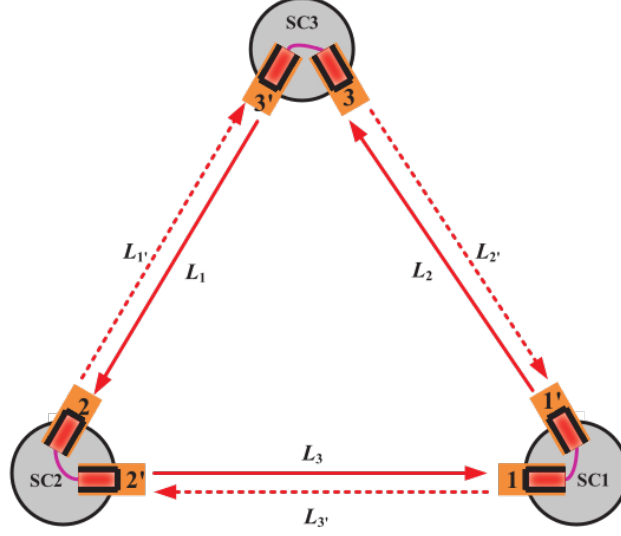


FIG. 1. A schematic diagram of the three-spacecraft constellation for the space-borne gravitational wave detector.

As shown in Fig. 1, a typical space-based gravitational wave detector is composed of a three-spacecraft constellation [5]. The armlength sitting on the opposite side of the spacecraft i (SCi) is denoted by L_i (and $L_{i'}$) with $i = 1, 2, 3$ in the counterclockwise (and clockwise) direction. On each spacecraft, two lasers are installed on the corresponding optical benches, labeled by i and i' . Three types of data streams, namely, the science data streams $s_{i(i')}$, test mass data streams $\epsilon_{i(i')}$, and reference data streams $\tau_{i(i')}$ are recorded by the phasemeters. The science data streams are the ones that carry the essential information on the gravitational waves, which triggers additional beat notes in the interference pattern. By the standard procedure of the TDI algorithm, the data streams are post-processed offline. The test mass and reference data streams are utilized to eliminate the optical bench motion noise. Following the standard procedure of the TDI algorithm, the optical bench motion noise can be eliminated, and two local lasers are effectively connected by intra-spacecraft phase locking [17]. The resultant observables read

$$\begin{aligned}\eta_i(t) &= H_i(t) + D_{i-1}p_{i+1}(t) - p_i(t) + \nu_{(i+1)'}\vec{n}_{i-1} \left[D_{i-1}\dot{\vec{\delta}}_{(i+1)'}(t) - \dot{\vec{\delta}}_i(t) \right] + N_i^{opt}(t), \\ \eta_{i'}(t) &= H_{i'}(t) + D_{(i+1)'}p_{i-1}(t) - p_{i'}(t) + \nu_{i-1}\vec{n}_{i+1} \cdot \left[\dot{\vec{\delta}}_{i'}(t) - D_{(i+1)'}\dot{\vec{\delta}}_{i-1}(t) \right] + N_{i'}^{opt}(t),\end{aligned}\quad (2)$$

where the laser frequency noise is denoted by p_i , $\dot{\vec{\delta}}_{i(i')}$ represents the test mass noise, $N_{i(i')}^{opt}$ gives the shot noise, $H_{i(i')}$ represent the gravitational wave signals, $D_{i(i')}$ are the time-delay operators along the related armlengths, and $\nu_{i(i')}$ are the laser's frequency. In terms of the observables $\eta_{i(i')}$, a valid TDI solution [5] aim to eliminate the laser frequency noise p_i by the combination

$$\text{TDI} = \sum_{i=1,2,3} (q_i\eta_i + q_{i'}\eta_{i'}), \quad (3)$$

where q_i and $q_{i'}$ are polynomials in the six time-delay operators. By focusing on the laser frequency noise and explicitly demanding the coefficients before individual p_i vanish, the above equation gives

$$\begin{aligned}q_1 + q_{1'} - q_{2'}D_{3'} - q_3D_2 &= 0, \\ q_2 + q_{2'} - q_{3'}D_{1'} - q_1D_3 &= 0, \\ q_3 + q_{3'} - q_{1'}D_{2'} - q_2D_1 &= 0.\end{aligned}\quad (4)$$

In particular, the Michelson-type TDI solution corresponds to when the communications between two spacecraft are interdicted. Without loss of generality, one assumes that the link connecting SC2 and SC3 is not working properly.

Therefore one has $\eta_2 = \eta_{3'} = 0$, or equivalently,

$$q_2 = q_{3'} = 0. \quad (5)$$

Substituting Eq. (5) into Eq. (4), and using two of the equations to eliminate $q_{2'}$ and q_3 , one finds

$$q_1(1 - D_{33'}) + q_{1'}(1 - D_{2'2}) = 0. \quad (6)$$

The above equation can be rewritten in a generalized form

$$\alpha(1 - a) + \beta(1 - b) = 0, \quad (7)$$

where $a \equiv D_{33'}$ and $b \equiv D_{2'2}$, and the unknown coefficients α and β are polynomials in a and b .

The combinatorial approach consists of the following key ingredients [15, 16]. One focuses on a particular class of commutators. The latter vanishes as long as the second-order terms regarding the time derivatives of the armlengths are ignored. It is shown that these commutators can be mapped to the residual laser noise of specific second-generation TDI combinations. Therefore, one systematically constructs the corresponding TDI solutions by adequately enumerating such commutators.

Specifically, one uses the subscript x to denote the first term of a commutator and y for the second term of the commutator. A particularly interesting communicator consists of two terms of the same size $[D_{x_1 x_2 \dots x_n}, D_{y_1 y_2 \dots y_n}]$, and the following relation is established [18]

$$[D_{x_1 x_2 \dots x_n}, D_{y_1 y_2 \dots y_n}] \phi(t) = \left(\sum_{i=1}^n L_{x_i} \sum_{j=1}^n \dot{L}_{y_j} - \sum_{j=1}^n L_{y_j} \sum_{i=1}^n \dot{L}_{x_i} \right) \dot{\phi} \left(t - \sum_{k=1}^n L_{x_k} - \sum_{k'=1}^n L_{y_{k'}} \right), \quad (8)$$

where a dot indicates the time derivative, and $\phi(t)$ is an arbitrary function of time. A proof of Eq. (8) is given in [16], which further generalizes to take into account time-advance operators $D_{\vec{i}, (\vec{i}')}$, so that the subscripts $x, y = i, i', \bar{i}, \bar{i}'$. Apparently, the first factor on the r.h.s. of Eq. (8) vanishes as long as

$$y_i = x_{\pi(i)}. \quad (9)$$

where $\pi \in \mathcal{S}_n$ is an element of the permutation group of degree n . In other words, Eq. (8) vanishes when $\{y_1 y_2 \dots y_n\}$ is an arbitrary permutation of $\{x_1 x_2 \dots x_n\}$. Moreover, as elaborated in [16], the difference between two monomials in a and b can be written as summation of multiplier of $(1 - a)$ or $(1 - b)$. As a result, the corresponding coefficients furnish a solution for α and β of Eq. (7), giving rise to a feasible TDI solution.

As an example, the Michelson-X combination can be derived by the commutator

$$\Delta = [ba, ab], \quad (10)$$

whose TDI coefficients reads

$$\begin{aligned} q_1 &= \alpha = 1 - b - ba + ab^2, \\ q_{1'} &= \beta = -(1 - a - ab + ba^2). \end{aligned} \quad (11)$$

III. THE SECOND-ORDER COMBINATORIAL ALGEBRAIC APPROACH

In this section, we first propose two novel classes of second-generation TDI solution by propositions 1, 2, and 3. In analogy to the algebraic approach discussed in the previous section, these solutions are also based on a particular form of commutator that vanishes. Unlike Eq. (8), the proposed formalisms are based on second-order commutators. Furthermore, we show that the solution space can be further expanded by using corollaries 1 and 2.

Proposition 1 *The following second-order commutator vanishes when the contributions associated with the second and higher-order time-derivatives are ignored*

$$\Delta_1 = [C, [A, B]], \quad (12)$$

where $A = \sum_i a_i$, $B = \sum_j b_j$, and $C = \sum_k c_k$ are arbitrary polynomials, and a_i, b_j, c_k are monomials, in the time-delay and time-advance operators.

Proposition 2 *The following product of first-order commutators vanishes when the contributions associated with the second and higher-order time-derivatives are ignored*

$$\Delta_2 = [C, D][A, B], \quad (13)$$

where A, B, C, D are polynomials.

More details regarding the proofs of propositions 1 and 2 are relegated to Appendix A.

Proposition 3 *A commutator constructed by employing either proposition 1 or 2 can always be written as a summation of multipliers of $(1 - a)$ or $(1 - b)$. Subsequently, the TDI coefficients can be derived.*

A general process for proposition 3 is given in Appendix B, closely follows the discussions in [16].

In what follows, we elaborate a few examples based on the above propositions. Regarding proposition 1, a Michelson-type solution for Eq. (7) reads

$$\Delta_1 = [a, [a, b]] = 2aba - a^2b - ab^2. \quad (14)$$

By noticing

$$\begin{aligned} aba &= -ab(1 - a) - a(1 - b) - (1 - a) + 1, \\ a^2b &= -a^2(1 - b) - a(1 - a) - (1 - a) + 1, \\ ba^2 &= -ba(1 - a) - b(1 - a) - (1 - b) + 1. \end{aligned} \quad (15)$$

Eq. (14) implies the following TDI coefficients

$$\begin{aligned} q_1 = \alpha &= -2ab - 2 + a + 1 + ba + b = -2ab + ba + a + b - 1, \\ q_{1'} = \beta &= -2a + a^2 + 1 = a^2 - 2a + 1. \end{aligned} \quad (16)$$

When compared against Michelson-X solution Eq. (10), the solution Eq. (14) involves three terms instead of two. Different from Eq. (8), the two terms of the commutator are not necessarily of equal length nor an equal number of factors, such as $[a, [a, ab]]$. Moreover, in its lowest order, Eq. (14) is featured by a compact size. To our knowledge, the solution Eq. (14) lies beyond the solution space explored in most literature, inclusively the preceding combinatorial algebraic algorithms.

An example of proposition 2 is

$$\Delta_2 = [a, b][a, b] = abab + baba - ab^2a - ba^2b. \quad (17)$$

By noticing

$$\begin{aligned} abab &= -aba(1 - b) - ab(1 - a) - a(1 - b) - (1 - a) + 1, \\ baba &= -bab(1 - a) - ba(1 - b) - b(1 - a) - (1 - b) + 1, \\ ab^2a &= -ab^2(1 - a) - ab(1 - b) - a(1 - b) - (1 - a) + 1, \\ ba^2b &= -ba^2(1 - b) - ba(1 - a) - b(1 - a) - (1 - b) + 1. \end{aligned} \quad (18)$$

Eq. (14) implies the following TDI coefficients

$$\begin{aligned} q_1 = \alpha &= -ab - 1 - bab - b + ab^2 + 1 + ab + b = ab^2 - bab - ab + ba, \\ q_{1'} = \beta &= -aba - a - ba - 1 + ab + a + ba^2 + 1 = -aba + ba^2 + ab - ba. \end{aligned} \quad (19)$$

Compared with the Michelson-X solution Eq. (10), the solution Eq. (17) double the number of terms of equal size. Again, in general, the terms involved in the commutator are not necessarily of equal length. Therefore the solution space is more significant than the first-order commutator approach. In its lowest order, the solution Eq. (17) is of equal size compared to the lowest-order second-generation geometric TDI ones. However, when one goes to a higher order, it may give rise to a trajectory featuring an odd count of total links, such as $[a, b][a, b^2]$, which is not included in Eq. (8) by definition. Moreover, the following corollaries expand the solution space while extending to the higher order cases.

Corollary 1 A higher-order commutator can be constructed by replacing the commutator $[A, B]$ in propositions 1 and 2 with a lower-order one formed using the propositions, namely,

$$\Delta_3 = [C, \Delta_1], \quad (20)$$

or

$$\Delta_3' = [C, D] \Delta_2. \quad (21)$$

The resulting commutator readily vanishes when the contributions associated with the second and higher-order time-derivatives are ignored.

Corollary 2 A commutator constructed by the linear combination of the commutators derived using the propositions 1 - 2 and corollary 1 vanishes when the contributions associated with the second and higher-order time-derivatives are ignored. Here, the coefficients of linear combination are defined as arbitrary polynomial of time-translation operators, which can be multiplied either to the left or to the right of the existing commutators.

An example of corollary 2 is

$$\Delta_4 = \Delta_2 - b\Delta_1 = abab + baba - ab^2a - ba^2b - b(2aba - a^2b - ab^2) = abab - baba - ab^2a + bab^2. \quad (22)$$

By noticing Eqs. (18) and

$$bab^2 = -bab(1 - b) - ba(1 - b) - b(1 - a) - (1 - b) + 1. \quad (23)$$

Eq. (22) implies the following TDI coefficients

$$\begin{aligned} q_1 = \alpha &= -ab - 1 + bab + b + ab^2 + 1 - ba - b = ab^2 + bab - ab - ba, \\ q_{1'} = \beta &= -aba - a + ba + 1 + ab + a - bab - 1 = -aba - bab + ab + ba. \end{aligned} \quad (24)$$

IV. APPLICATIONS TO DIFFERENT TYPES OF SECOND-ORDER TDI COMBINATIONS

In this section, we apply the proposed algorithm to TDI solutions of different types, such as the Monitor, Beacon, Relay, Sagnac, and full symmetric Sagnac ones. Besides, we elaborate on the corresponding sensitivity curves compared with the standard second-generation solutions. The specific forms of the response functions and residual noise power spectral densities are relegated to Appendix C. We will only focus on the two lowest-order solutions given by Eqs. (16) and (19). It is noted that higher-order solutions can be similarly constructed by employing the algorithm elaborated in the last section.

1. Michelson-type solutions

For the Michelson-type solutions, Eq. (16) gives

$$\begin{aligned} q_1 = \alpha &= -2D_{33'2'2} + D_{2'233'} + D_{33'} + D_{2'2} - 1, \\ q_{1'} = \beta &= D_{33'33'} - 2D_{33'} + 1, \end{aligned} \quad (25)$$

which gives rise to

$$\begin{aligned} X_{\Delta_1} &= (-2D_{33'2'2} + D_{2'233'} + D_{33'} + D_{2'2} - 1)\eta_1 + (D_{33'33'2'} - 2D_{33'2'} + D_{2'})\eta_3 \\ &\quad + (D_{33'33'} - 2D_{33'} + 1)\eta_{1'} + (-2D_{33'2'23} + D_{2'233'3} + D_{33'3} + D_{2'23} - D_3)\eta_{2'}. \end{aligned} \quad (26)$$

Similarly, Eq. (19) gives

$$\begin{aligned} q_1 = \alpha &= D_{33'2'22'2} + D_{2'233'} - D_{33'2'2} - D_{2'233'2'2}, \\ q_{1'} = \beta &= D_{2'233'33'} + D_{33'2'2} - D_{2'233'} - D_{33'2'233'}, \end{aligned} \quad (27)$$

which leads to

$$X_{\Delta_2} = (D_{33'2'22'2} + D_{2'233'} - D_{33'2'2} - D_{2'233'2'2})\eta_1 + (D_{2'233'33'2'} + D_{33'2'22'} - D_{2'233'2'} - D_{33'2'233'2'})\eta_3 \\ + (D_{2'233'33'} + D_{33'2'2} - D_{2'233'} - D_{33'2'233'})\eta_{1'} + (D_{33'2'22'23} + D_{2'233'3} - D_{33'2'23} - D_{2'233'2'23})\eta_{2'}. \quad (28)$$

Lastly, Eq. (24) gives

$$q_1 = -D_{33'2'2} + D_{33'2'22'2} + D_{2'233'2'2} + D_{2'2} - D_{2'22'233'} - D_{2'22'2}, \\ q_{1'} = -D_{33'2'233'} + D_{33'2'2} + D_{2'233'} - D_{2'2} \quad (29)$$

which leads to

$$X_{\Delta_4} = (-D_{33'2'2} + D_{33'2'22'2} + D_{2'233'2'2} + D_{2'2} - D_{2'22'233'} - D_{2'22'2})\eta_1 \\ + (-D_{33'2'233'2'} + D_{33'2'22'} + D_{2'233'2'} - D_{2'22'})\eta_3 \\ + (-D_{33'2'233'} + D_{33'2'2} + D_{2'233'} - D_{2'2})\eta_{1'} \\ + (-D_{33'2'23} + D_{33'2'22'23} + D_{2'233'2'23} + D_{2'23} - D_{2'22'233'3} - D_{2'22'23})\eta_{2'}. \quad (30)$$

Now we proceed to discuss the relation between the above solutions and those obtained by the standard geometric TDI approach. It is not difficult to verify that all three solutions can be obtained by the geometric TDI approach for a given link number using the method of exhaustion [14]. One might have expected that solution Eq. (26) belongs to the subset of ten-link geometric TDI combinations by simply counting the subscript indices of individual terms. However, as it turns out, it is a member of the twenty-link family. This is because the degree of a geodesic TDI solution is not necessarily governed by the term which contains the most subscript indices, as one might have to successively multiply the appropriate inverse operators from the left in order to retrieve the terms which correspond to the links suffering less time displacement operations. In other words, for a valid geometric TDI solution, the terminal time instant is not necessarily at $t = 0$ as long as the optical path encloses itself. On the other hand, it is observed that the degree of a geometric TDI solution must equate to the total number of terms. To be specific, the corresponding light propagation trajectories are shown in the space-time diagrams in Fig. 2.

To be more explicit, for X_{Δ_1} , its geometric TDI counterpart can be seen more transparently by rewriting Eq. (26) as

$$X_{\Delta_1} = -(\eta_1 + D_{33'}\eta_{2'} + D_{33'}\eta_{1'} + D_{33'2'}\eta_3 + D_{33'2'2}\eta_1 + D_{33'2'23}\eta_{2'}) \\ + (\eta_{1'} + D_{2'}\eta_3 + D_{2'2}\eta_1 + D_{2'23}\eta_{2'} + D_{2'233'}\eta_1 + D_{2'233'3}\eta_{2'}) \\ - (D_{33'}\eta_{1'} + D_{33'2'}\eta_3 + D_{33'2'2}\eta_1 + D_{33'2'23}\eta_{2'}) \\ + (D_{33'}\eta_1 + D_{33'3}\eta_{2'} + D_{33'33'}\eta_{1'} + D_{33'33'2'}\eta_3). \quad (31)$$

The corresponding light propagation trajectories are shown in the space-time diagrams in the top-left plot of Fig. 2. We note that the solution can be further decomposed into two first-generation combinations, corresponding to the first two and last two lines of Eq. (31). In particular, the data stream associated with the first line of Eq. (31) are indicated by the dashed blue line segments denoted by “(1)”-“(6)” shown in left subplot (a). The data stream associated with the second line of the equation are represented by the solid red line segments denoted by “1'”-“(6'”, also shown in the left subplot. It is apparent that these two six link trajectories form a closed trajectory. Similarly, the data stream associated with the third line of Eq. (31) are indicated by the dashed blue line segments denoted by “(1)”-“(4)” shown in the right subplot (b), where the dashed orange line segments correspond to additional time-displacements common to the data streams in question. The data stream associated with the fourth line of the equation are given by the solid red line segments denoted by “1'”-“(4'”, also shown in right subplot. Again, it is readily observed that the last two lines form a second closed trajectory. Similarly, the spacetime diagrams of the geometric TDI counterparts of the solutions X_{Δ_2} and X_{Δ_4} are also shown in Fig. 2.

The corresponding sensitivity curves are evaluated below in Appendix C and shown in Fig. 3 compared with the sixteen-link Michelson-X solution Eq. (11). It is observed that the sensitivity performance of the solution X_A^{20} is analytically identical to the Michelson-X one X_1^{16} [12].

2. Monitor-type solutions

Following the arguments given in [16], one considers the following two constraint equations for the second-generation Monitor-E combinations

$$q_3 = 0, q_{2'} = 0. \quad (32)$$

By substituting Eq. (32) into Eq. (4), and eliminating q_1 and $q_{1'}$, one finds

$$q_2(D_{\bar{3}} - D_{1\bar{2}'}) + q_{3'}(D_{\bar{2}'} - D_{1'\bar{3}}) = 0. \quad (33)$$

The above equation is essentially identical to Eq. (7) by recognizing $\alpha = q_2 D_{\bar{3}}$, $\beta = q_{3'} D_{\bar{2}'}$, $a = D_{31\bar{2}'}$, and $b = D_{2'1'\bar{3}}$.

For the commutator $[a, [a, b]]$, the corresponding TDI solution expressed in terms of the coefficients $q_2, q_{3'}$ reads

$$\begin{aligned} q_2 &= \alpha D_3 = -2D_{311'} + D_{2'1'1\bar{2}'3} + D_{31\bar{2}'3} + D_{2'1'} - D_3, \\ q_{3'} &= \beta D_{2'} = D_{31\bar{2}'31} - 2D_{31} + D_{2'}, \end{aligned} \quad (34)$$

which gives rise to

$$\begin{aligned} E_{\Delta_1} &= (D_{2'1'1\bar{2}'} + D_{31\bar{2}'} - D_{31\bar{2}'311'\bar{3}} - 1) \eta_1 + (-2D_{311'} + D_{2'1'1\bar{2}'3} + D_{31\bar{2}'3} + D_{2'1'} - D_3) \eta_2 \\ &\quad + (-D_{31\bar{2}'} + 1 + 2D_{311'1\bar{2}'} - D_{2'1'1\bar{2}'31\bar{2}'} - D_{2'1'1\bar{2}'}) \eta_{1'} + (D_{31\bar{2}'31} - 2D_{31} + D_{2'}) \eta_{3'}. \end{aligned} \quad (35)$$

Also, the solution corresponds to $[a, b][a, b]$ reads

$$\begin{aligned} q_2 &= \alpha D_3 = D_{311'\bar{3}2'1'} + D_{2'1'1\bar{2}'3} - D_{311'} - D_{2'1'11'}, \\ q_{3'} &= \beta D_{2'} = D_{2'1'1\bar{2}'31} + D_{311'\bar{3}2'} - D_{2'1'1} - D_{311'1}, \end{aligned} \quad (36)$$

which leads to

$$\begin{aligned} E_{\Delta_2} &= (D_{2'1'1\bar{2}'} - D_{311'\bar{3}} - D_{2'1'1\bar{2}'311'\bar{3}} + D_{311'11'\bar{3}}) \eta_1 + (D_{311'\bar{3}2'1'} + D_{2'1'1\bar{2}'3} - D_{311'} - D_{2'1'11'}) \eta_2 \\ &\quad + (D_{311'\bar{3}} - D_{2'1'1\bar{2}'} - D_{311'\bar{3}2'1'1\bar{2}'} + D_{2'1'11'1\bar{2}'}) \eta_{1'} + (D_{2'1'1\bar{2}'31} + D_{311'\bar{3}2'} - D_{2'1'1} - D_{311'1}) \eta_{3'}. \end{aligned} \quad (37)$$

We show in Fig. 3 the sensitivity curve which is found to be identical to the standard second-generation Monitor-E combination E_1^{16} [12].

3. Relay-type solutions

For the Relay type, we consider the following constraints

$$q_2 = 0, q_3 = 0. \quad (38)$$

which gives

$$q_{2'}(D_{\bar{3}} - D_{3'}) + q_{3'}(D_{\bar{2}'} - D_{1'\bar{3}}) = 0. \quad (39)$$

Again, it is equivalent to Eq. (7) by identifying $\alpha = q_{2'} D_{\bar{3}}$, $\beta = q_{3'} D_{\bar{2}'}$, $a = D_{33'}$ and $b = D_{2'1'\bar{3}}$.

For the commutator $[a, [a, b]]$, the corresponding TDI solution expressed in terms of the coefficients $q_{2'}, q_{3'}$ reads

$$\begin{aligned} q_{2'} &= \alpha D_3 = -2D_{33'2'1'} + D_{2'1'3'3} + D_{33'3} + D_{2'1'} - D_3, \\ q_{3'} &= \beta D_{2'} = D_{33'33'2'} - 2D_{33'2'} + D_{2'}, \end{aligned} \quad (40)$$

which gives rise to

$$\begin{aligned} U_{\Delta_1} &= (D_{2'1'3'} + D_{33'} - 1 - D_{33'33'2'1'\bar{3}}) \eta_1 + (D_{33'33'} - 2D_{33'} + 1) \eta_{1'} \\ &\quad + (-2D_{33'2'1'} + D_{2'1'3'3} + D_{33'3} + D_{2'1'} - D_3) \eta_{2'} + (D_{33'33'2'} - 2D_{33'2'} + D_{2'}) \eta_{3'}. \end{aligned} \quad (41)$$

Also, the solution corresponding to the commutator $[a, b][a, b]$ reads

$$\begin{aligned} q_{2'} &= \alpha D_3 = D_{33'2'1'\bar{3}2'1'} + D_{2'1'3'3} - D_{33'2'1'} - D_{2'1'3'2'1'}, \\ q_{3'} &= \beta D_{2'} = D_{2'1'3'33'2'} + D_{33'2'1'\bar{3}2'} - D_{2'1'3'2'} - D_{33'2'1'3'2'}, \end{aligned} \quad (42)$$

which leads to

$$\begin{aligned} U_{\Delta_2} &= (D_{2'1'3'} - D_{33'2'1'\bar{3}} - D_{2'1'3'33'2'1'\bar{3}} + D_{33'2'1'3'2'1'\bar{3}}) \eta_1 + (D_{2'1'3'33'} + D_{33'2'1'\bar{3}} - D_{2'1'3'} - D_{33'2'1'3'}) \eta_{1'} \\ &\quad + (D_{33'2'1'\bar{3}2'1'} + D_{2'1'3'3} - D_{33'2'1'} - D_{2'1'3'2'1'}) \eta_{2'} + (D_{2'1'3'33'2'} + D_{33'2'1'\bar{3}2'} - D_{2'1'3'2'} - D_{33'2'1'3'2'}) \eta_{3'}. \end{aligned} \quad (43)$$

We show in Fig. 3 the resulting sensitivity curve which is identical to that of the standard second-generation Relay combination U_1^{16} [12].

4. Beacon-type solutions

For the Beacon type, we consider the following constraints

$$q_3 = 0, q_{3'} = 0, \quad (44)$$

which gives

$$q_1(1 - D_{33'}) + q_{1'}(1 - D_{2'\bar{1}3'}) = 0. \quad (45)$$

Again, it is equivalent to Eq. (7) by identifying $a = D_{33'}$ and $b = D_{2'\bar{1}3'}$.

For the commutator $[a, [a, b]]$, the corresponding TDI solution expressed in terms of the coefficients $q_1, q_{1'}$ reads

$$\begin{aligned} q_1 &= \alpha = -2D_{33'2'\bar{1}3'} + D_{2'\bar{1}3'33'} + D_{33'} + D_{2'\bar{1}3'} - 1, \\ q_{1'} &= \beta = D_{33'33'} - 2D_{33'} + 1, \end{aligned} \quad (46)$$

which gives rise to

$$\begin{aligned} P_{\Delta_1} &= (-2D_{33'2'\bar{1}3'} + D_{2'\bar{1}3'33'} + D_{33'} + D_{2'\bar{1}3'} - 1) \eta_1 + (D_{33'33'} - 2D_{33'} + 1) \eta_{1'} \\ &\quad + (-D_{33'33'2'\bar{1}} + 2D_{33'2'\bar{1}} - D_{2'\bar{1}}) \eta_2 + (-2D_{33'2'\bar{1}3'3} + D_{2'\bar{1}3'33'3} + D_{33'3} + D_{2'\bar{1}3'3} - D_3 + D_{33'33'2'\bar{1}} - 2D_{33'2'\bar{1}} + D_{2'\bar{1}}) \eta_{2'}. \end{aligned} \quad (47)$$

On the other hand, the solution related to $[a, b][a, b]$ is found to be

$$\begin{aligned} q_1 &= \alpha = D_{33'2'\bar{1}3'2'\bar{1}3'} + D_{2'\bar{1}3'33'} - D_{33'2'\bar{1}3'} - D_{2'\bar{1}3'33'2'\bar{1}3'}, \\ q_{1'} &= \beta = D_{2'\bar{1}3'33'33'} + D_{33'2'\bar{1}3'} - D_{2'\bar{1}3'33'} - D_{33'2'\bar{1}3'33'}, \end{aligned} \quad (48)$$

which leads to

$$\begin{aligned} P_{\Delta_2} &= (D_{33'2'\bar{1}3'2'\bar{1}3'} + D_{2'\bar{1}3'33'} - D_{33'2'\bar{1}3'} - D_{2'\bar{1}3'33'2'\bar{1}3'}) \eta_1 \\ &\quad - (D_{2'\bar{1}3'33'33'2'\bar{1}} + D_{33'2'\bar{1}3'2'\bar{1}} - D_{2'\bar{1}3'33'2'\bar{1}} - D_{33'2'\bar{1}3'33'2'\bar{1}}) \eta_2 \\ &\quad + (D_{2'\bar{1}3'33'33'} + D_{33'2'\bar{1}3'} - D_{2'\bar{1}3'33'} - D_{33'2'\bar{1}3'33'}) \eta_{1'} \\ &\quad + \left[\begin{aligned} &(D_{33'2'\bar{1}3'2'\bar{1}3'3} + D_{2'\bar{1}3'33'3} - D_{33'2'\bar{1}3'3} - D_{2'\bar{1}3'33'2'\bar{1}3'3}) \\ &+ (D_{2'\bar{1}3'33'33'2'\bar{1}} + D_{33'2'\bar{1}3'2'\bar{1}} - D_{2'\bar{1}3'33'2'\bar{1}} - D_{33'2'\bar{1}3'33'2'\bar{1}}) \end{aligned} \right] \eta_{2'}. \end{aligned} \quad (49)$$

We show in Fig. 3 the sensitivity curve, which is again found to be identical to the standard second-generation Beacon combination P_1^{16} [12].

5. Sagnac-type solutions

For the Sagnac-alpha type, it is observed that the coefficients satisfy the following relations

$$q_2 = q_1 D_3, q_3 = q_1 D_{31}, q_{3'} = q_{1'} D_{2'}, q_{2'} = q_{1'} D_{2'1'}. \quad (50)$$

It is not difficult to show that two of the above equations are linearly dependent with Eqs. (4). To be specific, the relevant equation is obtained from the first line of Eqs. (4) by substituting the above conditions and eliminating $q_2, q_3, q_{2'}$, and $q_{3'}$. One finds

$$q_1(1 - D_{312}) + q_{1'}(1 - D_{2'1'3'}) = 0. \quad (51)$$

Again, it is equivalent to Eq. (7) by identifying $a = D_{312}$ and $b = D_{2'1'3'}$.

For the commutator $[a, [a, b]]$, the corresponding TDI solution expressed in terms of the coefficients $q_1, q_{1'}$ reads

$$\begin{aligned} q_1 = \alpha &= -2D_{3122'1'3'} + D_{2'1'3'312} + D_{312} + D_{2'1'3'} - 1, \\ q_{1'} = \beta &= D_{312312} - 2D_{312} + 1, \end{aligned} \quad (52)$$

which gives rise to

$$\begin{aligned} \alpha_{\Delta_1} &= (-2D_{3122'1'3'} + D_{2'1'3'312} + D_{312} + D_{2'1'3'} - 1) \eta_1 + (-2D_{3122'1'3'3} + D_{2'1'3'3123} + D_{3123} + D_{2'1'3'3} - D_3) \eta_2 \\ &\quad + (-2D_{3122'1'3'31} + D_{2'1'3'31231} + D_{31231} + D_{2'1'3'31} - D_{31}) \eta_3 + (D_{312312} - 2D_{312} + 1) \eta_{1'} \\ &\quad + (D_{3123122'1'} - 2D_{3122'1'} + D_{2'1'}) \eta_{2'} + (D_{3123122'} - 2D_{3122'} + D_{2'}) \eta_{3'}. \end{aligned} \quad (53)$$

Also, for the commutator $[a, b][a, b]$, the corresponding TDI solution reads

$$\begin{aligned} q_1 = \alpha &= D_{3122'1'3'2'1'3'} + D_{2'1'3'312} - D_{3122'1'3'} - D_{2'1'3'3122'1'3'}, \\ q_{1'} = \beta &= D_{2'1'3'312312} + D_{3122'1'3'} - D_{2'1'3'312} - D_{3122'1'3'312}, \end{aligned} \quad (54)$$

which leads to

$$\begin{aligned} \alpha_{\Delta_2} &= (D_{3122'1'3'2'1'3'} + D_{2'1'3'312} - D_{3122'1'3'} - D_{2'1'3'3122'1'3'}) \eta_1 \\ &\quad + (D_{3122'1'3'2'1'3'} + D_{2'1'3'312} - D_{3122'1'3'} - D_{2'1'3'3122'1'3'}) D_3 \eta_2 \\ &\quad + (D_{3122'1'3'2'1'3'} + D_{2'1'3'312} - D_{3122'1'3'} - D_{2'1'3'3122'1'3'}) D_{31} \eta_3 \\ &\quad + (D_{2'1'3'312312} + D_{3122'1'3'} - D_{2'1'3'312} - D_{3122'1'3'312}) \eta_{1'} \\ &\quad + (D_{2'1'3'312312} + D_{3122'1'3'} - D_{2'1'3'312} - D_{3122'1'3'312}) D_{2'1'} \eta_{2'} \\ &\quad + (D_{2'1'3'312312} + D_{3122'1'3'} - D_{2'1'3'312} - D_{3122'1'3'312}) D_{2'} \eta_{3'}. \end{aligned} \quad (55)$$

We show in Fig. 3 the sensitivity curve, compared against that of the standard second-generation Sagnac combination α_1^{16} [19].

6. Fully symmetric Sagnac-type solutions

For the fully-symmetric Sagnac type, we consider the following constraints

$$q_3 = -q_{3'}, q_2 = -q_{2'}, \quad (56)$$

which gives

$$q_1(1 - D_{3\bar{1}'2}) + q_{1'}(1 - D_{2'\bar{1}3'}) = 0. \quad (57)$$

Again, it is equivalent to Eq. (7) by identifying $a = D_{3\bar{1}'2}$ and $b = D_{2'\bar{1}3'}$.

For the commutator $[a, [a, b]]$, the corresponding TDI solution expressed in terms of the coefficients $q_1, q_{1'}$ reads

$$\begin{aligned} q_1 = \alpha &= -2D_{3\bar{1}'22'\bar{1}3'} + D_{2'\bar{1}3'3\bar{1}'2} + D_{3\bar{1}'2} + D_{2'\bar{1}3'} - 1, \\ q_{1'} = \beta &= D_{3\bar{1}'23\bar{1}'2} - 2D_{3\bar{1}'2} + 1, \end{aligned} \quad (58)$$

which gives rise to

$$\begin{aligned}\zeta_{\Delta_1} = & (-2D_{3\bar{1}'22'\bar{1}3'} + D_{2'\bar{1}3'3\bar{1}'2} + D_{3\bar{1}'2} + D_{2'\bar{1}3'} - 1)\eta_1 + (-D_{3\bar{1}'23\bar{1}'22'\bar{1}} + 2D_{3\bar{1}'22'\bar{1}} - D_{2'\bar{1}})\eta_2 \\ & - (2D_{3\bar{1}'22'\bar{1}3'3\bar{1}'} - D_{2'\bar{1}3'3\bar{1}'23\bar{1}'} - D_{3\bar{1}'23\bar{1}'} - D_{2'\bar{1}3'3\bar{1}'} + D_{3\bar{1}'})\eta_3 + (D_{3\bar{1}'23\bar{1}'2} - 2D_{3\bar{1}'2} + 1)\eta_{1'} \\ & - (-D_{3\bar{1}'23\bar{1}'22'\bar{1}} + 2D_{3\bar{1}'22'\bar{1}} - D_{2'\bar{1}})\eta_{2'} + (2D_{3\bar{1}'22'\bar{1}3'3\bar{1}'} - D_{2'\bar{1}3'3\bar{1}'23\bar{1}'} - D_{3\bar{1}'23\bar{1}'} - D_{2'\bar{1}3'3\bar{1}'} + D_{3\bar{1}'})\eta_{3'}. \quad (59)\end{aligned}$$

On the other hand, the commutator $[a, b][a, b]$ gives rise to the solution

$$\begin{aligned}q_1 = \alpha &= D_{3\bar{1}'22'\bar{1}3'2'\bar{1}3'} + D_{2'\bar{1}3'3\bar{1}'2} - D_{3\bar{1}'22'\bar{1}3'} - D_{2'\bar{1}3'3\bar{1}'22'\bar{1}3'}, \\ q_{1'} = \beta &= D_{2'\bar{1}3'3\bar{1}'23\bar{1}'2} + D_{3\bar{1}'22'\bar{1}3'} - D_{2'\bar{1}3'3\bar{1}'2} - D_{3\bar{1}'22'\bar{1}3'3\bar{1}'2},\end{aligned} \quad (60)$$

which leads to

$$\begin{aligned}\zeta_{\Delta_2} = & (D_{3\bar{1}'22'\bar{1}3'2'\bar{1}3'} + D_{2'\bar{1}3'3\bar{1}'2} - D_{3\bar{1}'22'\bar{1}3'} - D_{2'\bar{1}3'3\bar{1}'22'\bar{1}3'})\eta_1 \\ & - (D_{2'\bar{1}3'3\bar{1}'23\bar{1}'2} + D_{3\bar{1}'22'\bar{1}3'} - D_{2'\bar{1}3'3\bar{1}'2} - D_{3\bar{1}'22'\bar{1}3'3\bar{1}'2})D_{2'\bar{1}}\eta_2 \\ & - (D_{3\bar{1}'22'\bar{1}3'2'\bar{1}3'} + D_{2'\bar{1}3'3\bar{1}'2} - D_{3\bar{1}'22'\bar{1}3'} - D_{2'\bar{1}3'3\bar{1}'22'\bar{1}3'})D_{3\bar{1}'}\eta_3 \\ & + (D_{2'\bar{1}3'3\bar{1}'23\bar{1}'2} + D_{3\bar{1}'22'\bar{1}3'} - D_{2'\bar{1}3'3\bar{1}'2} - D_{3\bar{1}'22'\bar{1}3'3\bar{1}'2})\eta_{1'} \\ & + (D_{2'\bar{1}3'3\bar{1}'23\bar{1}'2} + D_{3\bar{1}'22'\bar{1}3'} - D_{2'\bar{1}3'3\bar{1}'2} - D_{3\bar{1}'22'\bar{1}3'3\bar{1}'2})D_{2'\bar{1}}\eta_{2'} \\ & + (D_{3\bar{1}'22'\bar{1}3'2'\bar{1}3'} + D_{2'\bar{1}3'3\bar{1}'2} - D_{3\bar{1}'22'\bar{1}3'} - D_{2'\bar{1}3'3\bar{1}'22'\bar{1}3'})D_{3\bar{1}'}\eta_{3'}.\end{aligned} \quad (61)$$

We show in Fig. 3 the sensitivity curve compared against that of the standard second-generation fully-symmetric Sagnac combination ξ_1^{16} [19].

7. Sagnac-inspired solutions

Last but not least, for the Sagnac-inspired type recently reported in [16], we consider the following constraints

$$q_1 = q_2 D_1, q_2 = q_3 D_2, \quad (62)$$

which gives

$$q_3(1 - A) + q_{3'}(1 - b) = 0. \quad (63)$$

It is equivalent to Eq. (7) by identifying $A = D_{2133'2'} - D_{23'2'} + D_{22'} - D_{212'} + D_{21} = \sum_i a_i$ and $b = D_{1'3'2'}$.

For the commutator $[A, [A, b]]$, the corresponding TDI solution expressed in terms of the coefficients $q_3, q_{3'}$ reads

$$\begin{aligned}q_3 = \alpha &= -2(D_{2133'2'} - D_{23'2'} + D_{22'} - D_{212'} + D_{21})D_{2133'2'} \\ &+ D_{1'3'2'}(D_{2133'2'} - D_{23'2'} + D_{22'} - D_{212'} + D_{21}) \\ &+ (D_{2133'2'} - D_{23'2'} + D_{22'} - D_{212'} + D_{21}) + D_{1'3'2'} - 1, \\ q_{3'} = \beta &= (D_{2133'2'} - D_{23'2'} + D_{22'} - D_{212'} + D_{21})(D_{2133'2'} - D_{23'2'} + D_{22'} - D_{212'} + D_{21}) \\ &- 2(D_{2133'2'} - D_{23'2'} + D_{22'} - D_{212'} + D_{21}) + 1,\end{aligned}$$

which gives rise to

$$\begin{aligned}
S_{\Delta_1} = & \left[\begin{aligned} & -2(D_{2133'2'} - D_{23'2'} + D_{22'} - D_{212'} + D_{21}) D_{2133'2'} + D_{1'3'2'} (D_{2133'2'} - D_{23'2'} + D_{22'} - D_{212'} + D_{21}) \\ & + (D_{2133'2'} - D_{23'2'} + D_{22'} - D_{212'} + D_{21}) + D_{1'3'2'} - 1 \end{aligned} \right] D_{21}\eta_1 \\
& + \left[\begin{aligned} & -2(D_{2133'2'} - D_{23'2'} + D_{22'} - D_{212'} + D_{21}) D_{2133'2'} + D_{1'3'2'} (D_{2133'2'} - D_{23'2'} + D_{22'} - D_{212'} + D_{21}) \\ & + (D_{2133'2'} - D_{23'2'} + D_{22'} - D_{212'} + D_{21}) + D_{1'3'2'} - 1 \end{aligned} \right] D_{21}\eta_2 \\
& + \left[\begin{aligned} & -2(D_{2133'2'} - D_{23'2'} + D_{22'} - D_{212'} + D_{21}) D_{2133'2'} + D_{1'3'2'} (D_{2133'2'} - D_{23'2'} + D_{22'} - D_{212'} + D_{21}) \\ & + (D_{2133'2'} - D_{23'2'} + D_{22'} - D_{212'} + D_{21}) + D_{1'3'2'} - 1 \end{aligned} \right] \eta_3 \\
& + \left\{ \begin{aligned} & \left[\begin{aligned} & (D_{2133'2'} - D_{23'2'} + D_{22'} - D_{212'} + D_{21})^2 - 2(D_{2133'2'} - D_{23'2'} + D_{22'} - D_{212'} + D_{21}) + 1 \end{aligned} \right] D_{1'} \\ & + \left[\begin{aligned} & -2(D_{2133'2'} - D_{23'2'} + D_{22'} - D_{212'} + D_{21}) D_{2133'2'} + D_{1'3'2'} (D_{2133'2'} - D_{23'2'} + D_{22'} - D_{212'} + D_{21}) \\ & + (D_{2133'2'} - D_{23'2'} + D_{22'} - D_{212'} + D_{21}) + D_{1'3'2'} - 1 \end{aligned} \right] D_{213} \end{aligned} \right\} D_{3'} \\
& - \left[\begin{aligned} & -2(D_{2133'2'} - D_{23'2'} + D_{22'} - D_{212'} + D_{21}) D_{2133'2'} + D_{1'3'2'} (D_{2133'2'} - D_{23'2'} + D_{22'} - D_{212'} + D_{21}) \\ & + (D_{2133'2'} - D_{23'2'} + D_{22'} - D_{212'} + D_{21}) + D_{1'3'2'} - 1 \end{aligned} \right] D_2 \\
& + \left[\begin{aligned} & -2(D_{2133'2'} - D_{23'2'} + D_{22'} - D_{212'} + D_{21}) D_{2133'2'} + D_{1'3'2'} (D_{2133'2'} - D_{23'2'} + D_{22'} - D_{212'} + D_{21}) \\ & + (D_{2133'2'} - D_{23'2'} + D_{22'} - D_{212'} + D_{21}) + D_{1'3'2'} - 1 \end{aligned} \right] D_2 \\
& - \left[\begin{aligned} & -2(D_{2133'2'} - D_{23'2'} + D_{22'} - D_{212'} + D_{21}) D_{2133'2'} + D_{1'3'2'} (D_{2133'2'} - D_{23'2'} + D_{22'} - D_{212'} + D_{21}) \\ & + (D_{2133'2'} - D_{23'2'} + D_{22'} - D_{212'} + D_{21}) + D_{1'3'2'} - 1 \end{aligned} \right] D_{21} \end{aligned} \right\} \\
& + \left[\begin{aligned} & (D_{2133'2'} - D_{23'2'} + D_{22'} - D_{212'} + D_{21})^2 - 2(D_{2133'2'} - D_{23'2'} + D_{22'} - D_{212'} + D_{21}) + 1 \end{aligned} \right] D_{1'} \\
& + \left[\begin{aligned} & -2(D_{2133'2'} - D_{23'2'} + D_{22'} - D_{212'} + D_{21}) D_{2133'2'} + D_{1'3'2'} (D_{2133'2'} - D_{23'2'} + D_{22'} - D_{212'} + D_{21}) \\ & + (D_{2133'2'} - D_{23'2'} + D_{22'} - D_{212'} + D_{21}) + D_{1'3'2'} - 1 \end{aligned} \right] D_{213} \\
& - \left[\begin{aligned} & -2(D_{2133'2'} - D_{23'2'} + D_{22'} - D_{212'} + D_{21}) D_{2133'2'} + D_{1'3'2'} (D_{2133'2'} - D_{23'2'} + D_{22'} - D_{212'} + D_{21}) \\ & + (D_{2133'2'} - D_{23'2'} + D_{22'} - D_{212'} + D_{21}) + D_{1'3'2'} - 1 \end{aligned} \right] D_2 \end{aligned} \right] \eta_2' \\
& + \left[(D_{2133'2'} - D_{23'2'} + D_{22'} - D_{212'} + D_{21})^2 - 2(D_{2133'2'} - D_{23'2'} + D_{22'} - D_{212'} + D_{21}) + 1 \right] \eta_3', \tag{64}
\end{aligned}$$

Similarly, the commutator $[A, b][A, b]$ gives rise to the solution

$$\begin{aligned}
q_3 = \alpha = & (D_{2133'2'1'3'2'1'3'2'} - D_{23'2'1'3'2'1'3'2'} + D_{22'1'3'2'1'3'2'} - D_{212'1'3'2'1'3'2'} + D_{211'3'2'1'3'2'}) \\
& + (D_{1'3'2'2133'2'} - D_{1'3'2'23'2'} + D_{1'3'2'22'} - D_{1'3'2'212'} + D_{1'3'2'21}) \\
& - (D_{2133'2'1'3'2'} - D_{23'2'1'3'2'} + D_{22'1'3'2'} - D_{212'1'3'2'} + D_{211'3'2'}) \\
& - (D_{1'3'2'2133'2'1'3'2'} - D_{1'3'2'23'2'1'3'2'} + D_{1'3'2'22'1'3'2'} - D_{1'3'2'212'1'3'2'} + D_{1'3'2'211'3'2'}), \\
q_3' = \beta = & D_{1'3'2'} (D_{2133'2'} - D_{23'2'} + D_{22'} - D_{212'} + D_{21})^2 \\
& + (D_{2133'2'1'3'2'} - D_{23'2'1'3'2'} + D_{22'1'3'2'} - D_{212'1'3'2'} + D_{211'3'2'}) \\
& - (D_{1'3'2'2133'2'} - D_{1'3'2'23'2'} + D_{1'3'2'22'} - D_{1'3'2'212'} + D_{1'3'2'21}) \\
& - (D_{2133'2'1'3'2'} - D_{23'2'1'3'2'} + D_{22'1'3'2'} - D_{212'1'3'2'} + D_{211'3'2'}) (D_{2133'2'} - D_{23'2'} + D_{22'} - D_{212'} + D_{21}),
\end{aligned}$$

which leads to

$$S_{\Delta_2} = q_1\eta_1 + q_2\eta_2 + q_3\eta_3 + q_1'\eta_1' + q_2'\eta_2' + q_3'\eta_3'. \tag{65}$$

where

$$q_2 = \left[\begin{aligned} & (D_{2133'2'1'3'2'1'3'2'} - D_{23'2'1'3'2'1'3'2'} + D_{22'1'3'2'1'3'2'} - D_{212'1'3'2'1'3'2'} + D_{211'3'2'1'3'2'}) \\ & + (D_{1'3'2'2133'2'} - D_{1'3'2'23'2'} + D_{1'3'2'22'} - D_{1'3'2'212'} + D_{1'3'2'21}) \\ & - (D_{2133'2'1'3'2'} - D_{23'2'1'3'2'} + D_{22'1'3'2'} - D_{212'1'3'2'} + D_{211'3'2'}) \\ & - (D_{1'3'2'2133'2'1'3'2'} - D_{1'3'2'23'2'1'3'2'} + D_{1'3'2'22'1'3'2'} - D_{1'3'2'212'1'3'2'} + D_{1'3'2'211'3'2'}) \end{aligned} \right] D_2, \tag{66}$$

$$\tag{67}$$

$$q_1 = \left[\begin{aligned} & (D_{2133'2'1'3'2'1'3'2'} - D_{23'2'1'3'2'1'3'2'} + D_{22'1'3'2'1'3'2'} - D_{212'1'3'2'1'3'2'} + D_{211'3'2'1'3'2'}) \\ & + (D_{1'3'2'2133'2'} - D_{1'3'2'23'2'} + D_{1'3'2'22'} - D_{1'3'2'212'} + D_{1'3'2'21}) \\ & - (D_{2133'2'1'3'2'} - D_{23'2'1'3'2'} + D_{22'1'3'2'} - D_{212'1'3'2'} + D_{211'3'2'}) \\ & - (D_{1'3'2'2133'2'1'3'2'} - D_{1'3'2'23'2'1'3'2'} + D_{1'3'2'22'1'3'2'} - D_{1'3'2'212'1'3'2'} + D_{1'3'2'211'3'2'}) \end{aligned} \right] D_{21}, \tag{68}$$

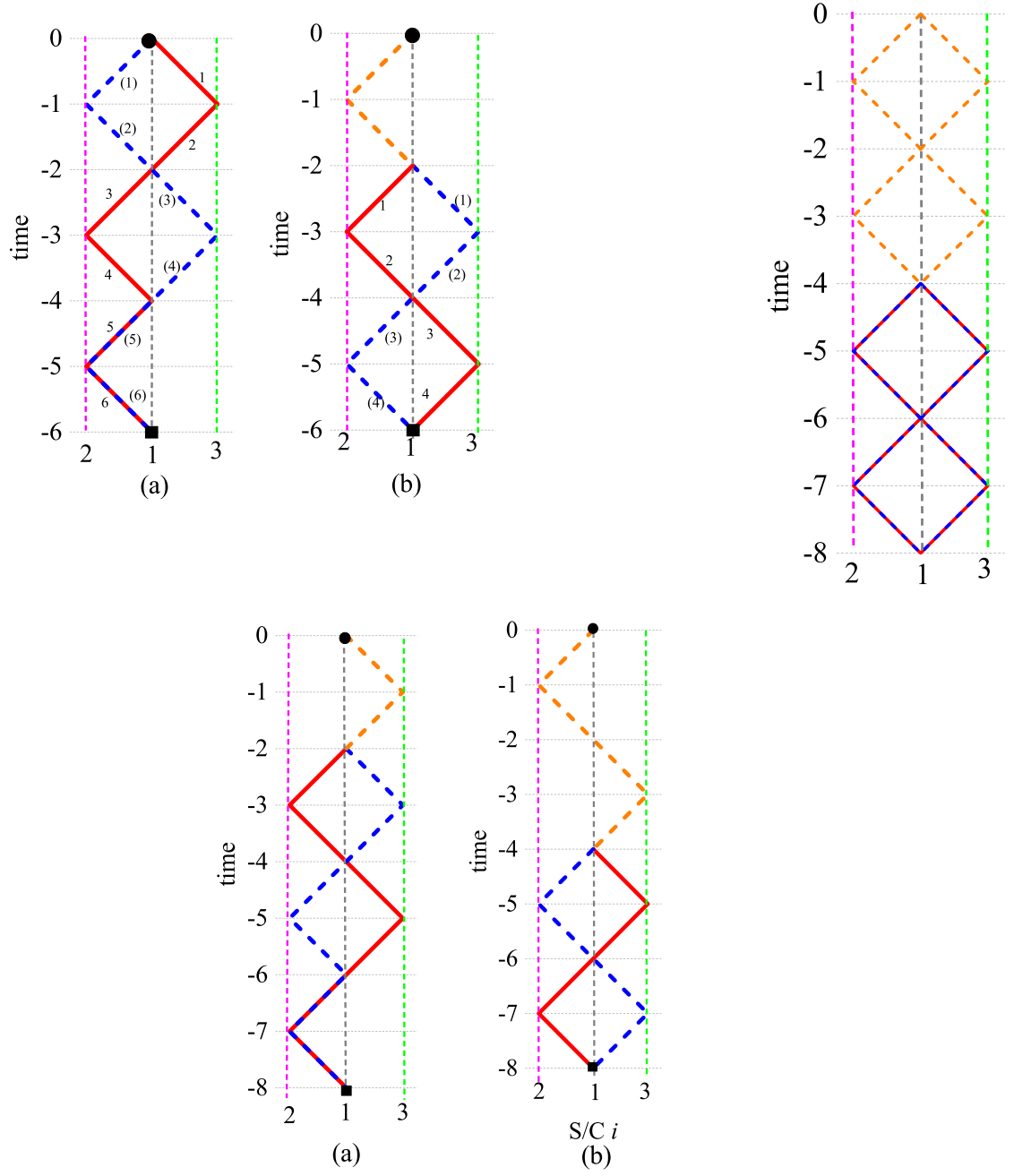


FIG. 2. The space-time diagrams for X_{Δ_1} (top left), X_{Δ_2} (bottom), and X_{Δ_4} (top right). The solid red and dashed blue line segments correspond to the two different light routes, while the dashed orange line segments indicate additional time-displacement operations common to the data streams in question.

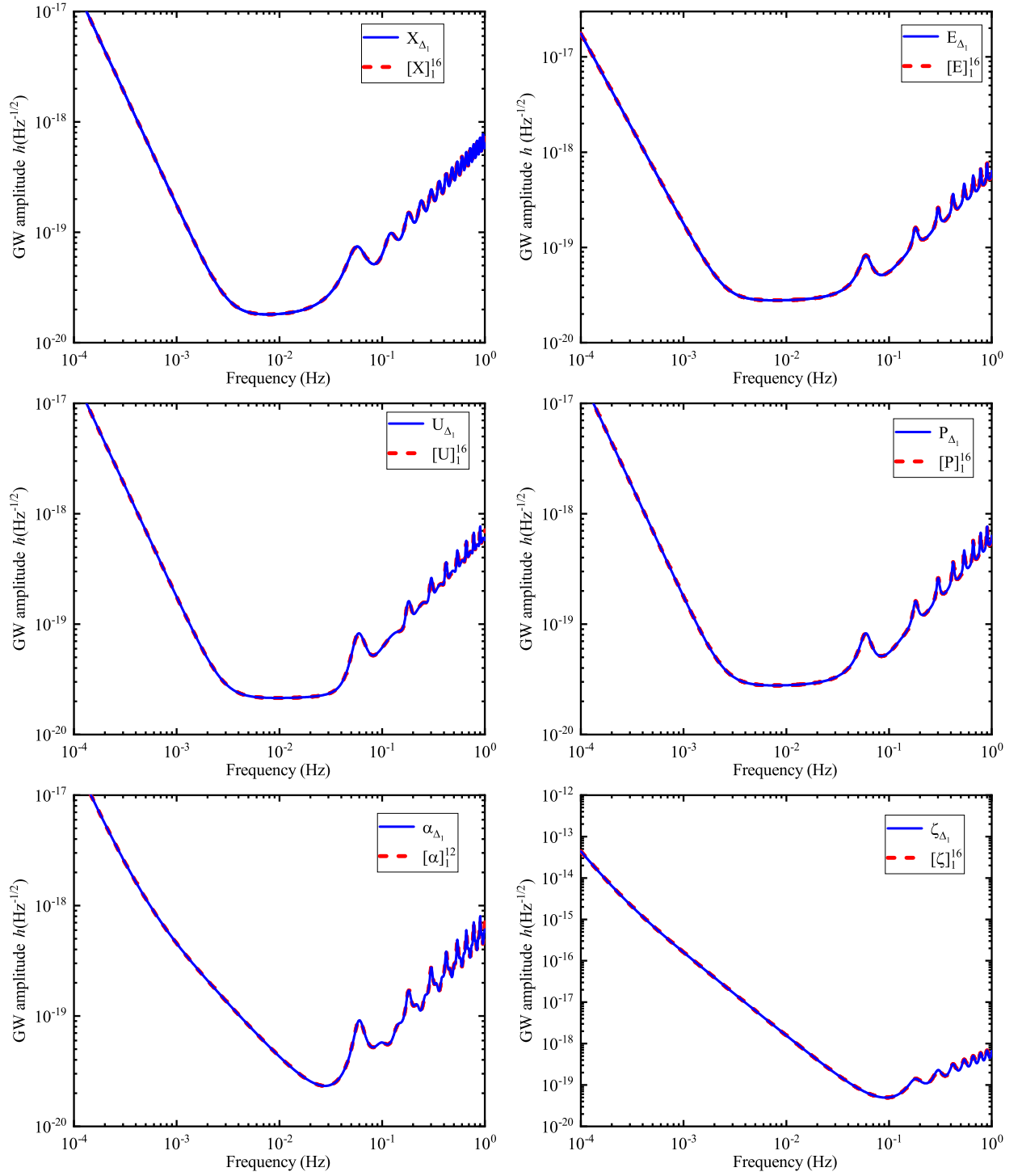


FIG. 3. The sensitivity curves for Michelson-X (top left), Monitor-E (top right), Beacon (middle left), Relay (middle right), Sagnac (bottom left), and fully-symmetric Sagnac (bottom right) type combinations obtained using the proposed algorithm. The solutions derived in this study are presented by solid blue curves, while the geometric TDI ones are shown in dashed red curves.

V. CONCLUDING REMARKS

The present study involves an attempt to enrich the TDI solutions from an algebraic perspective. Compared to the method of exhaustion, the advantage of an algebraic approach is its computational efficiency. Moreover, it paves the way to a better understanding of the relevant module of the non-commutative ring. The present study is motivated by further exploring the relationship between the commutators of the time-displacement operators and second-generation TDI combinations. Based on second-order commutators, we proposed an algebraic algorithm to seek the second-generation TDI combinations. The approach is based on a combinatorial algebraic scheme first introduced by Dhurandhar *et al.* and recently generalized by some of us by including the time-advance operator. In the present study, it is further generalized to a broadened solution space, essentially lying outside that of the geometric TDI approach. It is shown that novel second-generation solutions could be obtained for various TDI combinations, such as the Michelson, Monitor, Beacon, Relay, Sagnac, fully-symmetric Sagnac, and Sagnac-inspired ones. On the mathematical side, we generalized the vanishing condition of the original algorithm to a more general context by taking into account the time-advance operator and general polynomials.

Intuitively, a TDI solution extracted from a second-order commutator is expected to pay the “price” as it is often more extensive in size when compared to those derived from the first-order commutators. However, it is shown that the solutions are conveniently constructed by using commutators of rather compact form. Nonetheless, the present algorithm’s exhaustive nature is still unclear. Among others, the solution space is delimited by the specific constraint conditions, and subsequently, only specific subspaces have been explored. Lastly, as also pointed out by other authors, the major challenge of the algebraic approach for the second-generation TDI is owing to the non-commutative nature of the pertinent polynomial ring. A general algebraic approach, in this regard, should aim at furnishing the generators of the solution space. We plan to address these aspects in further studies.

ACKNOWLEDGEMENTS

We gratefully acknowledge the financial support from Brazilian agencies Fundação de Amparo à Pesquisa do Estado de São Paulo (FAPESP), Fundação de Amparo à Pesquisa do Estado do Rio de Janeiro (FAPERJ), Conselho Nacional de Desenvolvimento Científico e Tecnológico (CNPq), and Coordenação de Aperfeiçoamento de Pessoal de Nível Superior (CAPES). This work is also supported by the National Natural Science Foundation of China (Grant No.11925503), the Postdoctoral Science Foundation of China (Grant No.2022M711259), Guangdong Major project of Basic and Applied Basic Research (Grant No.2019B030302001), Natural Science Foundation of Hubei Province (2021CFB019), and the Fundamental Research Funds for the Central Universities, HUST: 2172019kfyRCPY029.

Appendix A: The properties of the proposed commutators

In this Appendix, we elaborate on the proofs of propositions 1 and 2 given in the main text.

Since polynomials are composed of monomials, and due to the relations

$$\begin{aligned} &= [a, b] + [a, c], \\ [a + b, c] &= [a, c] + [b, c], \end{aligned}$$

for arbitrary monomials a, b , and c , one only needs to show that propositions 1 and 2 are correct for arbitrary monomials.

A crucial feature of the present scheme is that one also needs to deal with the inverse of the time-delay operator, namely, the time-advance operators that satisfying

$$D_{\bar{i}}D_i = D_iD_{\bar{i}} = \mathcal{I}, \quad (\text{A1})$$

where \mathcal{I} is the identity operator.

When applied to an arbitrary time-dependent variable $\phi(t)$, we have

$$D_{\bar{i}}\phi(t) = \phi(t + L_i(t + L_i)), \quad (\text{A2})$$

where one ignores the second-order terms, which can be expanded to give

$$\begin{aligned} D_i \phi(t) &\simeq \phi(t + L_i) + \dot{\phi}(t + L_i)(t + L_i) \dot{L}_i \\ &= \phi(t + L_i) + \dot{\phi}(t + L_i) t \dot{L}_i + \dot{\phi}(t + L_i) L_i \dot{L}_i. \end{aligned} \quad (\text{A3})$$

In [16], one shows the following generalized form of Eq. (8)

$$[D_{x_1 x_2 \dots x_n}, D_{y_1 y_2 \dots y_n}] \phi(t) = \left(\sum_{i=1}^n \delta_{x_i} L_{x_i} \sum_{j=1}^n \delta_{y_j} \dot{L}_{y_j} - \sum_{j=1}^n \delta_{y_j} L_{y_j} \sum_{i=1}^n \delta_{x_i} \dot{L}_{x_i} \right) \dot{\phi} \left(t - \sum_{k=1}^n \delta_{x_k} L_{x_k} - \sum_{k'=1}^n \delta_{y_{k'}} L_{y_{k'}} \right), \quad (\text{A4})$$

where

$$\begin{aligned} \delta_{x_k} &= \begin{cases} -1 & \text{if } k = i \text{ for any } i = \mu_1, \dots, \mu_l, \\ +1 & \text{otherwise} \end{cases}, \\ \delta_{y_{k'}} &= \begin{cases} -1 & \text{if } k' = j \text{ for any } j = \nu_1, \dots, \nu_m, \\ +1 & \text{otherwise} \end{cases}, \end{aligned} \quad (\text{A5})$$

where one assumes that there are l instances of time-advance operators in $D_{x_1 x_2 \dots x_n}$ and m instances in $D_{y_1 y_2 \dots y_n}$. The subscripts of those time-advance operators are denoted by μ_i with $i = 1, \dots, l$ and ν_j with $j = 1, \dots, m$.

Apparently, the vanishing condition Eq. (9) remains unchanged when the time-advance is considered. However, two arbitrary monomials, a and b , do not necessarily have the same length. For $n \neq m$,

$$\Delta(n, m) \sim [D_{x_1 x_2 \dots x_n}, D_{y_1 y_2 \dots y_m}] \quad (\text{A6})$$

where “ \sim ” indicates the lengths of the two elements of the commutator, Eq. (A4) cannot be utilized straightforwardly. Nonetheless, for $n = m$, Eq. (A4) leads to

$$[a, b\Delta(n, m)c]\phi(t) \sim ab[D_{x_1 x_2 \dots x_n}, D_{y_1 y_2 \dots y_n}]c\phi(t) - b[D_{x_1 x_2 \dots x_n}, D_{y_1 y_2 \dots y_n}]ca\phi(t) = 0, \quad (\text{A7})$$

for arbitrary monomials a, b , and c .

On the other hand, for the lowest-order commutators

$$[a_1, b_1 c_1] = [a_1, b_1]c_1 + b_1[a_1, c_1] \sim \Delta[1, 1]c_1 + b_1\Delta[1, 1],$$

and

$$\begin{aligned} [a_1 d_1 e_1, b_1 c_1] &= [a_1, b_1 c_1]d_1 e_1 + a_1[d_1 e_1, b_1 c_1] = [a_1, b_1]c_1 d_1 e_1 + b_1[a_1, c_1]d_1 e_1 + a_1[d_1 e_1, b_1 c_1] \\ &\sim \Delta[1, 1]c_1 d_1 e_1 + b_1\Delta[1, 1]d_1 e_1 + a_1\Delta[2, 2], \end{aligned}$$

where a_1, b_1 , and c_1 are monomials of degree one. In both cases, the r.h.s. of the equation are written into the summation of some particular $\Delta(i, i)$ multipliers. The latter is formed by multiplying, from either left and right, by some monomials.

$$[A, B] \sim \sum_i a_i \Delta(n_i, n_i) b_i. \quad (\text{A8})$$

Although somewhat tedious, it is straightforward to show by *mathematical induction* that Eq. (A8) is general. By putting the above two pieces together, one finds that Δ_1 defined by proposition 1 indeed vanishes.

Now, for proposition 2, one employs Eq. (A8) for both commutators $[A, B]$ and $[C, D]$. Then it is straightforward to observe that all the terms in the resultant expression are proportional to the form $\dot{L}_x \dot{L}_y$, which is subsequently ignored in the context of second-generation TDI.

The proofs of proposition 3 and corollary 1 and 2 are apparent.

Appendix B: The procedure to map a commutator to the associated TDI solution

Because a polynomial is composed of monomials, one rewrites the monomial as a summation of multipliers in either $(1 - a)$ or $(1 - b)$. To achieve this, one performs successive long division of individual monomial by either $(1 - a)$ or

$(1 - b)$ from the right. It is not difficult to show that the last remainder is always “1”.

For individual monomial t_n , its decomposition can be carried out as follows, reminiscent of the procedure discussed in [16].

1. Initiate $\lambda = 0$ and $\gamma = 0$
2. It is noted that t_n ends in either a , \bar{a} , b , or \bar{b} , namely, $t_n = t_{n-1}a$, $t_n = t_{n-1}\bar{a}$, $t_n = t_{n-1}b$, or $t_n = t_{n-1}\bar{b}$.
 - If $t_n = t_{n-1}a$, let $\lambda = \lambda - t_{n-1}$;
 - If $t_n = t_{n-1}\bar{a}$, let $\lambda = \lambda + t_{n-1}\bar{a}$;
 - If $t_n = t_{n-1}b$, let $\gamma = \gamma - t_{n-1}$;
 - If $t_n = t_{n-1}\bar{b}$, let $\gamma = \gamma + t_{n-1}\bar{b}$;
3. Repeat the above procedure 2 for t_{n-1} , until the degree of the monomial vanishes, namely, t_0 . We note that $t_0 = 1$.
4. We have $t_n = \lambda(1 - a) + \gamma(1 - b) + 1$.

As an example, for the case $t_4 = ba\bar{b}a$, we have $t_3 = ba\bar{b}$, $t_2 = ba$, $t_1 = b$, $t_0 = 1$. So that $\lambda = -t_3 - t_1 = -ba\bar{b} - b$ and $\gamma = t_2\bar{b} + t_0 = ba\bar{b} + 1$, and subsequently, $ba\bar{b}a = -ba\bar{b}(1 - a) + ba\bar{b}(1 - b) - b(1 - a) - (1 - b) + 1$. Since a constructed commutator by the process always involves an even number of monomials with successively flipped signs, the t_0 terms are guaranteed to be entirely canceled out.

Appendix C: Sensitivity funtions for the novel combinations

This Appendix presents the expressions for the averaged response functions of gravitational waves and noise power spectral density for the combinations elaborated in the main text.

For the Michelson-type combination, the noise power spectral density $N_X(u)$ is expressed as

$$N_X(u) = 64 (3 + \cos [2u]) \sin [u]^4 \times \frac{L^2 s_a^2}{u^2 c^4} + 64 \sin [u]^4 \times \frac{u^2 s_x^2}{L^2}, \quad (\text{C1})$$

and the gravitational waves averaged response function $R_X(u)$ reads

$$R_X(u) = -\frac{8(12 - 15 \cos [u] + 12 \cos [2u]) \sin [u]^4}{3u^2} - \frac{8 \sin [u]^4 (15 \sin [u] - 24 \cos [u] \sin [u])}{3u^3} - \frac{8 \sin [u]^4 (21 \sin [u] - 6 \sin [2u])}{3u} \\ - \frac{8}{3} \sin [u]^4 \left[\begin{array}{l} -5 - \cos [2u] + 18 \cos [2u] (\text{Ci} [u] - 2\text{Ci} [2u] + \text{Ci} [3u] + \log [\frac{4}{3}]) \\ -12 (\text{Ci} [u] - \text{Ci} [2u] + \log [2]) + 18 \sin [2u] (\text{Si} [u] - 2\text{Si} [2u] + \text{Si} [3u]) \end{array} \right].$$

where $u = 2\pi f c/L$ and f is observed frequency, SinIntegral $\text{Si}(z) = \int_0^z \sin t/t dt$ and CosIntegral $\text{Ci}(z) = -\int_z^\infty \cos t/t dt$.

For the Monitor-type combination, the noise power spectral density $N_E(u)$ is expressed as

$$N_E(u) = 64 (3 + \cos [u]) \sin \left[\frac{u}{2} \right]^4 \times \frac{L^2 s_a^2}{u^2 c^4} + 32 (3 + 2 \cos [u]) \sin \left[\frac{u}{2} \right]^4 \times \frac{u^2 s_x^2}{L^2}, \quad (\text{C2})$$

and the gravitational waves averaged response function $R_E(u)$ reads

$$R_E(u) = \frac{2(-33 + 45 \cos [u] - 33 \cos [2u] - 15 \cos [3u]) \sin \left[\frac{u}{2} \right]^4}{3u^2} \\ + \frac{2 \sin \left[\frac{u}{2} \right]^4 (-81 \sin [u] + 27 \sin [2u] - 3 \sin [3u])}{3u} + \frac{2 \sin \left[\frac{u}{2} \right]^4 (-75 \sin [u] + 33 \sin [2u] + 15 \sin [3u])}{3u^3} \\ + \frac{2}{3} \sin \left[\frac{u}{2} \right]^4 \left[\begin{array}{l} 20 + 4 \cos [u] + 168 (1 + \cos [u]) \text{Ci} [u] - 240 (1 + \cos [u]) \text{Ci} [2u] + \\ 24 (3 (1 + \cos [u]) \text{Ci} [3u] + (1 + \cos [u]) \log [\frac{1024}{27}] + 3 \sin [u] (\text{Si} [u] - 2\text{Si} [2u] + \text{Si} [3u])) \end{array} \right].$$

For the Relay-type combination, the noise power spectral density $N_U(u)$ is expressed as

$$N_E(u) = 256 \cos \left[\frac{u}{2} \right]^2 (5 + 5 \cos [u] + 2 \cos [2u]) \sin \left[\frac{u}{2} \right]^4 \times \frac{L^2 s_a^2}{u^2 c^4} \\ + 128 \cos \left[\frac{u}{2} \right]^2 (4 + 4 \cos [u] + \cos [2u]) \sin \left[\frac{u}{2} \right]^4 \times \frac{u^2 s_x^2}{L^2}, \quad (\text{C3})$$

and the gravitational waves averaged response function $R_U(u)$ reads

$$R_U(u) = \frac{4 \cos \left[\frac{u}{2} \right]^2 (-87 + 36 \cos [u] - 102 \cos [2u] - 48 \cos [3u] - 15 \cos [4u]) \sin \left[\frac{u}{2} \right]^4}{3u^2} \\ + \frac{4 \cos \left[\frac{u}{2} \right]^2 \sin \left[\frac{u}{2} \right]^4 (-324 \sin [u] + 24 (\sin [2u] + \sin [3u]) - 3 \sin [4u])}{3u} \\ + \frac{4 \cos \left[\frac{u}{2} \right]^2 \sin \left[\frac{u}{2} \right]^4 (-132 \sin [u] + 72 \sin [2u] + 48 \sin [3u] + 15 \sin [4u])}{3u^3} \\ + \frac{4}{3} \cos \left[\frac{u}{2} \right]^2 \sin \left[\frac{u}{2} \right]^4 \left\{ \begin{aligned} &72 + 56 \cos [u] + 16 \cos [2u] \\ &+ 48 \left[\begin{aligned} &(7 + 6 \cos [u] - \cos [2u]) \text{Ci} [u] - 2 (5 + 3 \cos [u] - 2 \cos [2u]) \text{Ci} [2u] + \cos [2u] \log \left[\frac{27}{16} \right] \\ &+ \log \left[\frac{1024}{27} \right] + \cos [u] \log [64] + 6 \text{Ci} [3u] \sin [u]^2 \\ &- 3 (\sin [u] + \sin [2u]) (\text{Si} [u] - 2 \text{Si} [2u] + \text{Si} [3u]) \end{aligned} \right] \end{aligned} \right\}.$$

For the Beacon-type combination, the noise power spectral density $N_P(u)$ is expressed as

$$N_P(u) = 256 \cos \left[\frac{u}{2} \right]^2 (3 + \cos [u]) \sin \left[\frac{u}{2} \right]^4 \times \frac{L^2 s_a^2}{u^2 c^4} + 32 (3 + 2 \cos [u]) \sin \left[\frac{u}{2} \right]^2 \sin [u]^2 \times \frac{u^2 s_x^2}{L^2}, \quad (\text{C4})$$

and the gravitational waves averaged response function $R_P(u)$ reads

$$R_P(u) = \frac{8 \cos \left[\frac{u}{2} \right]^2 (-33 + 45 \cos [u] - 33 \cos [2u] - 15 \cos [3u]) \sin \left[\frac{u}{2} \right]^4}{3u^2} \\ + \frac{8 \cos \left[\frac{u}{2} \right]^2 \sin \left[\frac{u}{2} \right]^4 (-81 \sin [u] + 27 \sin [2u] - 3 \sin [3u])}{3u} \\ + \frac{8 \cos \left[\frac{u}{2} \right]^2 \sin \left[\frac{u}{2} \right]^4 (-75 \sin [u] + 33 \sin [2u] + 15 \sin [3u])}{3u^3} \\ + \frac{8}{3} \cos \left[\frac{u}{2} \right]^2 \sin \left[\frac{u}{2} \right]^4 \left[\begin{aligned} &20 + 4 \cos [u] + 168 (1 + \cos [u]) \text{Ci} [u] - 240 (1 + \cos [u]) \text{Ci} [2u] + \\ &24 (3 (1 + \cos [u]) \text{Ci} [3u] + (1 + \cos [u]) \log \left[\frac{1024}{27} \right] + 3 \sin [u] (\text{Si} [u] - 2 \text{Si} [2u] + \text{Si} [3u])) \end{aligned} \right].$$

For the Sagnac- α -type combination, the noise power spectral density $N_\alpha(u)$ is expressed as

$$N_\alpha(u) = 128 (1 + 2 \cos [u])^4 (5 + 4 \cos [u] + 2 \cos [2u]) \sin \left[\frac{u}{2} \right]^6 \times \frac{L^2 s_a^2}{u^2 c^4} + 96 \sin \left[\frac{3u}{2} \right]^4 \times \frac{u^2 s_x^2}{L^2}, \quad (\text{C5})$$

and the gravitational waves averaged response function $R_\alpha(u)$ reads

$$R_\alpha(u) = \frac{2 \left(-72 \sin \left[\frac{u}{2} \right]^2 + 180 \cos [u] \sin \left[\frac{u}{2} \right]^2 - 72 \cos [2u] \sin \left[\frac{u}{2} \right]^2 \right) \sin \left[\frac{3u}{2} \right]^4}{3u^2} \\ + \frac{2 \sin \left[\frac{3u}{2} \right]^4 \left(-180 \sin \left[\frac{u}{2} \right]^2 \sin [u] + 72 \sin \left[\frac{u}{2} \right]^2 \sin [2u] \right)}{3u^3} \\ + \frac{2 \sin \left[\frac{3u}{2} \right]^4 (-204 \sin [u] + 147 \sin [2u] - 30 \sin [3u])}{3u} \\ + \frac{2}{3} \sin \left[\frac{3u}{2} \right]^4 \left\{ \begin{aligned} & 24 (8 + 4 \cos [u] + 3 \cos [3u]) \text{Ci} [u] - 48 (7 + 2 \cos [u] + 3 \cos [3u]) \text{Ci} [2u] \\ & + 72 \sin \left[\frac{u}{2} \right]^2 + 32 \cos [u] \sin \left[\frac{u}{2} \right]^2 + 16 \cos [2u] \sin \left[\frac{u}{2} \right]^2 \\ & + 24 \left[6 \text{Ci} [3u] + 6 \log \left[\frac{4}{3} \right] + 3 \cos [3u] (\text{Ci} [3u] + \log \left[\frac{4}{3} \right]) + \right. \\ & \left. \log [4] + \cos [u] \log [16] + 3 \sin [3u] (\text{Si} [u] - 2 \text{Si} [2u] + \text{Si} [3u]) \right] \end{aligned} \right\}.$$

For the fully-symmetric Sagnac type combination, the noise power spectral density $N_\zeta(u)$ is expressed as

$$N_\zeta(u) = 6e^{-3iu} (-1 + e^{iu})^4 (-1 + 2e^{iu}) \times \frac{L^2 s_a^2}{u^2 c^4} \\ + [6 (5 - 6 \cos [u] + \cos [2u] - 2i (-1 + \cos [u]) \sin [u])] \times \frac{u^2 s_x^2}{L^2}, \quad (\text{C6})$$

and the gravitational waves averaged response function $R_{zeta\alpha}(u)$ reads

$$R_\zeta(u) = \frac{1}{u^3} e^{-\frac{iu}{2}} \left(\cos \left[\frac{u}{2} \right] + 3i \sin \left[\frac{u}{2} \right] \right) \sin \left[\frac{u}{2} \right]^2 \times \\ \left[\begin{aligned} & 12u^3 (2 + 3 \cos [u]) \text{Ci} [u] - 24u^3 (1 + 3 \cos [u]) \text{Ci} [2u] \\ & + 36u^3 \cos [u] \text{Ci} [3u] + 36u^3 \cos [u] \log \left[\frac{4}{3} \right] + 12u^3 \log [4] + 4u^3 \sin \left[\frac{u}{2} \right]^2 + \\ & 30u \cos [u] \sin \left[\frac{u}{2} \right]^2 + 3u^2 \sin [u] - 3u^2 \cos [u] \sin [u] - 30 \sin \left[\frac{u}{2} \right]^2 \sin [u] \\ & + 36u^3 \sin [u] \text{Si} [u] - 72u^3 \sin [u] \text{Si} [2u] + 36u^3 \sin [u] \text{Si} [3u] \end{aligned} \right].$$

For all the above cases, the resultant sensitivity function reads

$$S(u) = \frac{\sqrt{N(u)}}{\sqrt{\frac{2}{5}} \sqrt{R(u)}}. \quad (\text{C7})$$

The plots shown in Fig. 3 are evaluated using Eqs. (C1)–(C7).

-
- [1] M. Tinto and J. W. Armstrong, *Physical Review D* **59**, 102003 (1999).
 - [2] P. Amaro-Seoane *et al.*, arXiv preprint arXiv:1702.00786 (2017).
 - [3] J. Luo *et al.*, *Classical and Quantum Gravity* **33**, 035010 (2016), arXiv: 1512.02076.
 - [4] W.-R. Hu and Y.-L. Wu, *National Science Review* **4**, 685 (2017).
 - [5] M. Tinto and S. V. Dhurandhar, *Living Reviews in Relativity* **24**, 1 (2021).
 - [6] M. Vallisneri, *Physical Review D* **72**, 042003 (2005).
 - [7] J. W. Armstrong, F. B. Estabrook, and M. Tinto, *The Astrophysical Journal* **527**, 814 (1999).
 - [8] N. J. Cornish and R. W. Hellings, *Classical and Quantum Gravity* **20**, 4851 (2003).
 - [9] S. V. Dhurandhar, K. R. Nayak, and J.-Y. Vinet, *Physical Review D* **65**, 102002 (2002).
 - [10] K. R. Nayak and J.-Y. Vinet, *Physical Review D* **70**, 102003 (2004).
 - [11] D. Cox, J. Little, and D. OShea, *Ideals, varieties, and algorithms: an introduction to computational algebraic geometry and commutative algebra* (Springer Science & Business Media, 2013).
 - [12] M. Tinto, F. B. Estabrook, and J. W. Armstrong, *Physical Review D* **69**, 082001 (2004).
 - [13] O. Hartwig and M. Muratore, *Phys. Rev. D* **105**, 062006 (2022).
 - [14] P.-P. Wang, W.-L. Qian, Y.-J. Tan, H.-Z. Wu, and C.-G. Shao, *Phys. Rev. D* **106**, 024003 (2022).
 - [15] S. V. Dhurandhar, K. R. Nayak, and J.-Y. Vinet, *Classical and Quantum Gravity* **27**, 135013 (2010).
 - [16] Z.-Q. Wu, P.-P. Wang, W.-L. Qian, and C.-G. Shao, (2022), arXiv:2210.07801.
 - [17] M. Tinto and O. Hartwig, *Physical Review D* **98**, 042003 (2018).

- [18] S. V. Dhurandhar, Journal of Physics: Conference Series **154**, 012047 (2009).
- [19] M. Otto, *Time-Delay Interferometry Simulations for the Laser Interferometer Space Antenna*, PhD thesis, Leibniz Universität Hannover, 2015.